Accuracy of Vertical Deflection Determination by Present-Day Inertial Instrumentation

K. P. Schwarz
Department of Surveying Engineering, University of New Brunswick
Fredericton, N.B., Canada E3B 5A3

Abstract. The conventional procedures to determine deflections of the vertical in mountainous terrain require time-consuming astronomical or gravimetric methods and their application is therefore restricted to a small number of stations. The interpolation of vertical deflections between such stations can be performed by the Inertial Surveying System currently used for position determination. The principle of such a procedure is outlined and the existing implementations are discussed.

An analysis of results obtained in the Canadian Rocky Mountains indicates that the observation of deflection differences along the same line can be repeated with a precision of about 0".5 but that there are systematic discrepancies between the forward and the backward running of the same line. A comparison with the available astronomically determined deflections also shows systematic differences of 2" to 3". These errors are most likely due to the 'overshooting' of the Kalman procedure at gradient changes. It appears that the software can be altered in such a way that deflection differences between stations, not more than half an hour of travel time apart, can be determined by the inertial system with an accuracy of better than ± 1".

1. Introduction

Two methods have conventionally been used to determine the deflections of the vertical ξ and η which define the difference in direction between the ellipsoidal normal and the actual gravity vector. The first approach uses integral formulas to determine the deflection components from gravity anomalies Δg. In Vening-Meinesz' integral

$$\begin{Bmatrix}\xi\\ \eta\end{Bmatrix} = \frac{1}{4\pi G}\iint_{\sigma} \Delta g \frac{dS}{d\psi}\begin{Bmatrix}\cos\alpha\\ \sin\alpha\end{Bmatrix} d\sigma \qquad (1.1)$$

ξ and η are in principal computed at the surface of the geoid. Here G denotes a mean value of gravity for the whole earth, $S(\psi)$ is Stokes' function, ψ is the spherical distance, α is the azimuth, and σ indicates integration over the earth. In Molodenski's approach ξ and η are determined at the earth's surface. The second method uses astronomically determined latitude and longitude (Φ, Λ) and geodetic latitude and longitude (ϕ,λ) to obtain deflection components at the observation point by the simple relations

$$\begin{aligned}\xi &= \Phi - \phi\\ \eta &= (\Lambda - \lambda)\cos\phi\end{aligned} \qquad (1.2)$$

Usually, the deflection coverage of larger areas is rather sparse because of the time-consuming data acquisition procedures. This is especially true for mountainous terrain where a dense coverage would be required to adequately represent the slope changes of the equipotential surfaces. The amount of work required for this is prohibitive in most cases. Methods to interpolate deflections between stations where the gravity vectors are known are therefore of great interest. Two ways to approach this problem have evolved in recent years. They could be called computational and observational interpolation. In the first approach all information about the anomalous gravity field in a certain area is combined to predict deflection values at the specific point. Methods differ as to the way in which the different data groups are combined and represented. But all have in common that they employ heterogeneous data and thus avoid the limitations which are often encountered when using one type of observations only. The actual resolution of these methods depends to a large extent upon the amount, the accuracy, and the distribution of the data. With a scarce coverage as for instance in mountainous areas it is impossible to recover any details. While this approach is characterized by the optimal use of the available information, the second approach relies on an instrument which is capable of measuring changes of the direction of the gravity vector with reference to an initial point. In this case a detailed mapping of the deflection changes along the path of the instrument is possible. Thus, a relative geoid can be computed which is then oriented by the absolute deflection values obtained by other means. Inertial systemsare capable of performing such an observational interpolation and from their error characteristics an application in mountainous terrain seems to be especially promising.

The discussion will concentrate on deflection interpolation with such instruments. This limited application should not obstruct the view for one of the main advantages of these systems: the capability to obtain position and gravity field information at the same time. It seems that because of historic subdivisions in geodesy the full potential of inertial systems is not yet utilized.

The following sections will be somewhat biased towards the Litton 'Inertial Surveying System'. This does not indicate a preference but has been dictated by the fact that the only data available to the author had been taken with this system.

2. Movement of an Inertial System in a Local Gravitational Field

An inertial measuring unit consists basically of three mutually orthogonal accelerometers and of an assembly of gyroscopes establishing a reference frame with known orientation to the accelerometer triad. Usually, the accelerometers will

Proc. of the 9th GEOP Conference, *An International Symposium on the Applications of Geodesy to Geodynamics, October 2-5, 1978.* Dept. of Geodetic Science Rept. No. 280. The Ohio State Univ., Columbus, Ohio 43210.

be aligned along the output axes of the gyros. The output of the accelerometer triad are three components of specific force

$$f_i = \ddot{r}_i + g_i \qquad (2.1)$$

where $\ddot{r}_i$ are the inertially referenced accelerations expressed as the second derivatives of a radius vector with respect to time and g_i are the components of the gravitational acceleration at the system location due to all bodies in the universe. For surveys on the surface of the earth the origin of the inertial system is usually translated to the mass center of the earth thereby making the variations of the gravitational effect of all extra-terrestrial bodies smaller than 2.10^{-7}. Thus, for relative accuracies of about 2.10^{-7} only the effect of the earth's gravitational field has to be considered. Since the measuring accuracy of available inertial systems is of the order of 10^{-5} an earth centered origin will be assumed hereafter.

The accelerometer triad can be related to the inertial triad by connecting the two radius vectors by a rotation matrix C

$$r^I = Cr^A \qquad (2.2)$$

where the superscripts I and A refer to the inertial and to the accelerometer frame respectively. Differentiating twice with respect to time we obtain

$$\ddot{r}^I = C\ddot{r}^A + 2C\dot{r}^A + C\ddot{r}^A \qquad (2.3)$$

We now can distinguish three special cases. If C is independent of time,only the first term on the right-hand side remains and equation (2.3) expresses the rotation between two inertial frames. Such a system can be instrumented by mounting the accelerometers on a gimballed platform and keeping its orientation fixed in inertial space. These systems are called space stabilized. Honeywell's Geo-spin is a system developed along these lines for geodetic purposes. In the second case the only time dependency allowed in C will be the rotation of the earth. Such a system will again make use of a gimballed platform which now will be constantly torqued in such a way that it stays orthogonal to a reference ellipsoid. These systems are called local-level and can directly be related to the geodetic (ϕ, λ, h) - coordinates; Litton's 'Inertial Surveying System' and Ferranti's system work with this concept. If finally an arbitrary time dependency is allowed in C, equation (2.3) represents a strapdown system. In this case the inertial instruments are mounted along axes attached to the vehicle and the orientation changes arbitrarily with respect to inertial space. So far, systems of this kind have not been developed for geodetic applications.

The principle of inertial geodesy can best be seen from equation (2.1). If the gravity vector g_i is known we can obtain position by integrating twice

$$\ddot{r}_i = f_i - g_i \qquad (2.1a)$$

Usually, only an approximation to g_i is available, either in form of the normal gravity vector γ_i or in form of a higher order approximation from one of the satellite solutions. In that case the differences between the reference field and the actual field can be determined by measurement using the normal case as a first approximation. Thus, position and gravity field determination become intertwined in an iterative procedure. This concept will be used in the sequel for a local-level system.

Another approach which shows clearly the interdependence of geometry and physics starts from the holonomity problem. The transformation of locally imperfect differentials into locally perfect differentials for frames used in geodesy has been discussed in detail by Grafarend (1975).

The specific force equation for a local-level system is obtained from equation (2.1) and (2.3)

$$f_i = C\ddot{r}_i^A + 2C\dot{r}_i^A + C\ddot{r}_i^A + g_i \qquad (2.4)$$

The first three members on the right-hand side are usually expressed in terms of vehicle velocity, earth rotation rate, and ellipsoidal radii (see e.g. Britting, 1971). The important point is that an ellipsoidal surface is used for all computations and that small correction terms are applied to account for the deviations between model and reality. This is done by splitting the gravity vector g into a normal and an anomalous part

$$g_i = \gamma_i + \delta g_i \qquad (2.5)$$

or

$$\text{grad } W = \text{grad } U + \text{grad } T \qquad (2.6)$$

where W is the gravity potential, U is the normal ellipsoidal gravity potential, and T is the anomalous gravitational potential. Similarly, g_i is the gravity vector, γ_i the normal gravity vector, and δg_i the gravity disturbance vector. The vectors are now expressed in spherical coordinates with geocentric latitude $\bar{\phi}$, longitude λ, and radius vector r. Using the usual series expansion of the normal potential U (see e.g. Heiskanen and Moritz (1967), p. 230), we obtain

$$U = \frac{kM}{r}\{1 - \sum_{n=1}^{\infty} J_{2n}\left(\frac{a}{r}\right)^{2n} P_{2n}(\sin\bar{\phi})\} + \psi(r,\bar{\phi}) \qquad (2.7)$$

where

$$J_{2n} = (-1)^{n+1}\frac{3e^{2n}}{(2n+1)(2n+3)}\left(1-n+5n\frac{C-A}{ME^2}\right),$$

kM is the gravitational constant times the mass of the earth, J_{2n} are the even harmonic coefficients of the expansion, a is the semi-major axis of the ellipsoid, $P_{2n}(\sin\phi)$ are Legendre polynomials, E is the linear eccentricity $E = (a^2 - b^2)^{1/2}$, e is the first eccentricity $e=E/a$, C and A are the earth's moments of inertia around its axis of rotation and around an axis in the equatorial plane respectively, and $\psi(r, \phi)$ is the centrifugal potential. We then have

$$\gamma = \text{grad } U = \frac{1}{r}\frac{\partial U}{\partial \bar{\phi}} i_{\bar{\phi}} + \frac{1}{r \cos\bar{\phi}}\frac{\partial U}{\partial \lambda} i_{\lambda} + \frac{\partial U}{\partial r} i_r \quad (2.8)$$

where

$$\frac{\partial U}{\partial \lambda} = 0$$

because of rotational symmetry. The other two partial derivatives are

$$\frac{1}{r}\frac{\partial U}{\partial \bar{\phi}} = \gamma_{\bar{\phi}} = \frac{kM}{r^2}\sum_{n=1}^{\infty} J_{2n}\left(\frac{a}{r}\right)^{2n} P'_{2n}(\sin\bar{\phi}) + \frac{\partial \psi}{\partial \bar{\phi}} \quad (2.9)$$

where

$$P'_{2n}(\sin\bar{\phi}) = -\cos\bar{\phi}\sum_{k=1}^{n}(4n - 4k + 3) \cdot P_{2n-2k+1}(\sin\bar{\phi})$$

and

$$\frac{\partial U}{\partial r} = \gamma_r = -\frac{kM}{r^2}\{1 - \sum_{n=1}^{\infty}(1 + 2n) J_{2n}\left(\frac{a}{r}\right)^{2n} \cdot P_{2n}(\sin\bar{\phi}) + \frac{\partial \psi}{\partial r} \quad (2.10)$$

Since the series (2.9) and (2.10) converge very fast approximations of the form

$$\gamma_{\bar{\phi}} = \gamma_e (a_1 + a_2 \sin^2\bar{\phi}) \sin\bar{\phi}\cos\bar{\phi} \quad (2.11)$$

and

$$\gamma_r = \gamma_e (1 + b_1 \sin^2\bar{\phi} + b_2 \sin^4\bar{\phi}) \quad (2.12)$$

can be used where γ_e refers to normal gravity at the equator. The coefficients a_1, a_2, b_1, b_2 depend on the reference system chosen. The relative accuracy of these formulas is about 10^{-8}. With the same accuracy normal gravity along the ellipsoidal normal γ_n can be obtained by using

$$\gamma_n = \gamma_{\bar{\phi}} \sin\varepsilon - \gamma_r \cos\varepsilon \quad (2.13)$$

where $\varepsilon = 0.50\, e^2 \sin 2\phi$.

The absence of odd degree terms in formula (2.7) is necessary in order to maintain the same ellipsoidal reference surface for all computations. An inclusion of the J_3 - term as for instance in (Britting, 1971) is inconsistent with the use of the ellipsoid as a computational surface. If higher order approximations are used for the gravity field, formulas for the appropriate surfaces must be developed.

Conceptually, the anomalous part of the gravity field can be treated in exactly the same way as the normal part. Using the expansion of the anomalous potential T into spherical harmonics

$$T = \frac{kM}{r}\{1 - \sum_{n=2}^{\infty}\left(\frac{a}{r}\right)^n J'_n P_n(\sin\phi) - \sum_{n=2}^{\infty}\sum_{m=1}^{n}\left(\frac{a}{r}\right)^n (J_{nm}\cos m\lambda + K_{nm}\sin m\lambda) \cdot P_{nm}(\sin\phi)\} \quad (2.14)$$

where J'_n are the zonal coefficients minus the normal part and J_{nm}, K_{nm} are the tesseral harmonic coefficients, we can again differentiate with respect to ϕ, λ, and r. There are, however, two difficulties with this approach. First, only truncated series (2.14) are available from satellite observations which will not give the required local details. Second, the evaluation of such series will be too laborious for real time computations. For the following discussion we will therefore assume that only the normal part of the gravity field as represented by equations (2.7) to (2.13) is known.

Equation (2.5) shows that the deviations from the normal model are given by the gravity disturbance vector δg_i which has the components

$$\begin{bmatrix} \delta g_{\phi} \\ \delta g_{\lambda} \\ \delta g_r \end{bmatrix} = \begin{bmatrix} \frac{1}{r}\frac{\partial T}{\partial \phi} \\ \frac{1}{r\cos\phi}\frac{\partial T}{\partial \lambda} \\ \frac{\partial T}{\partial r} \end{bmatrix} \quad (2.15)$$

Using spherical approximations the right-hand side can be expressed in terms of ξ, η, and Δg

$$\begin{bmatrix} \delta g_{\phi} \\ \delta g_{\lambda} \\ \delta g_r \end{bmatrix} = \begin{bmatrix} -\gamma_o \xi \\ -\gamma_o \eta \\ \Delta g + \frac{2G}{R} N \end{bmatrix} \quad (2.16)$$

where γ_o denotes normal gravity at the ellipsoid, G and R are mean values of gravity and earth radius respectively, and N is the geoidal undulation at the point.

Changes of these quantities from one station to the next can be determined by using two properties of an inertial system: the capability to align to the local vertical and the faculty to keep an orientation fixed in space. The first property allows determination of the direction of the local gravity vector each time the system stops. The second property makes it possible to transport an orthogonal frame established at an initial point to other points on the earth's surface and to use it as a reference. Thus, the actual changes of the gravity vector can be compared to the changes of the normal gravity vector i.e. changes of the gravity disturbance vector (2.16) can be determined. If the gravity vector is known at the initial point it can be determined in all subsequent points. Strictly speaking, an iterative process would be required, expressing the fact that position and gravity field determination cannot be separated. In practice, the iterative corrections will often be negligible because of the small distances between stations.

It should be well understood that the changes of the gravity disturbance vector are not continuously recorded but can only be determined at discrete points where the vehicle stops. For continuous recording gradiometers must be added to the inertial system. However, it is of interest for the following discussion to relate the gravity disturbance vector to changes in the gravity field and in vehicle motion. A derivation of the relevant formulas is given in (Moritz 1975). Using the notations

$$T_i = \frac{\partial T}{\partial X_i} \qquad T_{ij} = \frac{\partial^2 T}{\partial X_i \, \partial X_j}$$

we can write

$$T_i(t) = T_i^0 + \int_{t_o}^{t} T_{ij}(s) \{u_i^o - \int_{t_o}^{s} \bar{f}_j(r)\, dr + \int_{t_o}^{s} T_j(r)\, dr\}\, ds \,, \tag{2.17}$$

where

$$\bar{f}_j = f_j - \gamma_j \,,$$

u denotes the velocity, and the superscript zero indicates an initial value. The last term on the right of formula (2.17) describes the interaction between gravitation and inertia. Since its effect will be very small in the applications considered here, it will be neglected hereafter. This approximation does not affect the following argument. Using the relations (2.14) and (2.15) results in

$$\begin{aligned}
\xi &\approx \xi_o + \frac{1}{\gamma_o r} \int_{t_o}^{t} (T_{\phi\phi} v_\phi + T_{\phi\lambda} v_\lambda + T_{\phi r} v_r)\, ds \\
\eta &\approx \eta_o + \frac{1}{\gamma_o r \cos\phi} \int_{t_o}^{t} (T_{\lambda\phi} v_\phi + T_{\lambda\lambda} v_\lambda + T_{\lambda r} v_r)\, ds \\
\Delta g &= \Delta g_o - \int_{t_o}^{t} (T_{r\phi} v_\phi + T_{r\lambda} v_\lambda + T_{rr} v_r)\, ds + \\
&\quad + \frac{2G}{R}(N_o - N) \,,
\end{aligned} \tag{2.18}$$

where

$$v_i = \int_{t_o}^{t} \bar{f}_i(s)\, ds$$

because of $u_i^o = 0$. For local applications the term with $(N^i - N_o)$ can be neglected. Except for small corrections the v_i represent the velocity components and with

$$v_r << (v_\lambda, v_\phi)$$

in many cases the deflections of the vertical can be expressed by the approximation

$$\begin{aligned}
\xi &= \xi_o + \frac{1}{\gamma_o r} \int_{t_o}^{t} (T_{\phi\phi} v_\phi + T_{\phi\lambda} v_\lambda)\, ds \\
\eta &= \eta_o + \frac{1}{\gamma_o r \cos\phi} \int_{t_o}^{t} (T_{\lambda\phi} v_\phi + T_{\lambda\lambda} v_\lambda)\, ds \,.
\end{aligned} \tag{2.19}$$

This formula shows that changes in ξ and η are dependent on the ratio v_ϕ / v_λ, i.e. on the instrument heading. This is especially apparent for an L-shaped traverse which first runs east - west and then south - north. We obtain

$$\Delta\xi_{E-W} = \frac{1}{\gamma_o r} \int_{t_o}^{t} T_{\phi\lambda} v_\lambda\, ds$$

$$\Delta\xi_{S-N} = \frac{1}{\gamma_o r} \int_{t_o}^{t} T_{\phi\phi} v_\phi\, ds$$

and

$$\Delta\eta_{E-W} = \frac{1}{\gamma_o r \cos\phi} \int_{t_o}^{t} T_{\lambda\lambda} v_\lambda\, ds$$

$$\Delta\eta_{S-N} = \frac{1}{\gamma_o r \cos\phi} \int_{t_o}^{t} T_{\lambda\phi} v_\phi\, ds.$$

3. Implementation of the Measuring Principle in the Inertial Surveying System

Fig. 3.1 ilustrates the principle of determining changes in the gravity disturbance vector by an inertial measuring unit. At an initial point P_1 the system is aligned to the local gravity vector g_1 by a levelling procedure which drives the two 'horizontal' velocity outputs to zero and by establishing astronomical north via gryocompassing. Basically, a local astronomical (Φ,Λ) - system is established. The small angle θ_i between g_i and γ_i is called the total deflection of the vertical. The initial frame is transported to P_2 making corrections for the rotation rate of the earth by continuously torquing the platform. Similarly, compensation of changes of the normal gravity vector are included in the specific force equation. At P_2 the changes of the gravity disturbance vector will cause a small misalignment of the platform with respect to the local vertical and the resulting velocity readings in the 'horizontal' accelerometers can be resolved into the components $\Delta\xi$ and $\Delta\eta$.

At this point two different procedures are possible. The first one is used in the 'Rapid Geodetic Survey System' (RGSS) and is illustrated in fig. 3.2. In this case the velocity readings are recorded but the initial frame is left unchanged, i.e. only the above mentioned torques and normal gravity corrections are applied. The reference surface for the computations is then an ellipsoid which is slightly tilted against the global reference ellipsoid because the alignment has been made with respect to the local vertical. If ϕ, λ, h, ξ, and η are known in the initial point this tilt can theoretically be removed. Since this system measures differences in ellip-

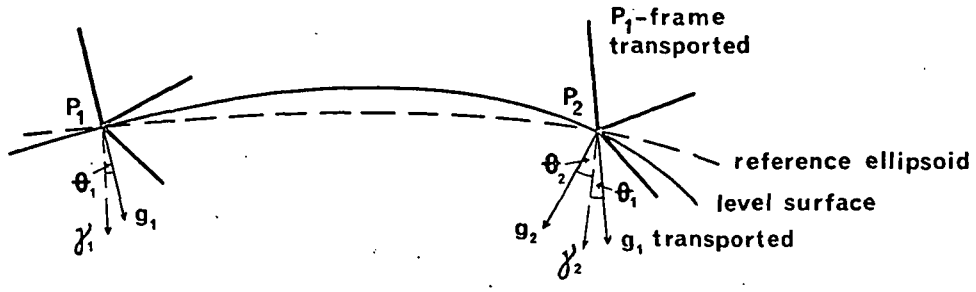

Fig. 3.1 Principle of measuring deflection changes

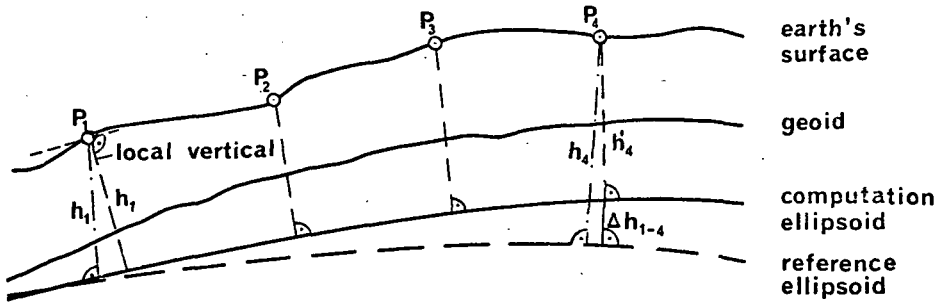

Fig. 3.2 Principle of 'Rapid Geodetic Survey System'

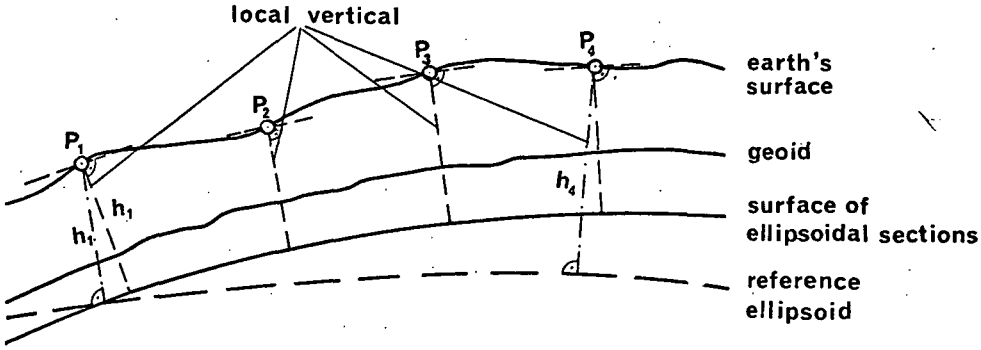

Fig. 3.3 Principle of 'Inertial Positioning System'

soidal height h it is also possible to use the deviation between measured and known height difference Δh_{1-4} to retilt the ellipsoid. By using the deflection information provided at the zero updates the changes of the geoidal undulation between P_1 and P_4 can be computed.

The second procedure is used in the 'Inertial Positioning System' (IPS) and is illustrated in fig. 3.3. In this case the frame is realigned to the local vertical at each zero update. This means that the geoid is approximated by a sequence of ellipsoidal sections. The height differences determined from this surface will approximate levelled height differences. The interpretation of the computed latitude and longitude differences is somewhat problematic.

Theoretically, the anholonomity problem creeps in at this point. Practically, a piecewise mapping onto the ellipsoid will give results which are acceptable within the limits of present measuring accuracy. With improved systems this procedure should, however, be avoided.

So far, measuring errors have not been considered. They will disturb the simple relations discussed above. Certain error sources produce accelerations which are very similar to those generated by changes in the gravity field. A separation can be achieved by an adequate measuring process. Changes in the gravity field are position dependent, at least at the level of accuracy considered here, while most instrumental errors are time dependent. A well designed survey can help to separate the two disturbances. Reoccupation of stations after certain time intervals and checks at stations with a known gravity disturbance vector will provide a control of the instrumental errors.

The present 'Inertial Surveying System' controls the different error sources by a hierarchy of biases. They are either added to the specific force equations or used to modify the torquing commands. In this concept the gravity disturbances are considered as one of several sources of noise. Optimal filtering techniques are used to eliminate this noise. Thus, deflection changes are absorbed

into bias changes. The separation from instrumental errors, especially gyro drift, is done under the assumption that the correlation functions are known. Two sets of biases are important for deflection determination: the alignment biases and the Kalman biases.

The first group, consisting of three gyro biases and one accelerometer bias, is determined during the levelling and gyrocompassing procedure at the initial point and remains constant for one mission. It fixes the tilt of the computation surface against the global reference ellipsoid and also introduces a scale factor in the height computation. Since a number of different effects are lumped into the gyro biases the resulting tilt cannot be considered as representing the gravity disturbances at the initial point. This will have a second-order effect on the computation of deflection differences but will in general be negligible for local applications.

The second group of biases, the Kalman biases, are determined at each zero update. In this case, the value of each bias b_i is recomputed using the new data x (velocities) according to a priori knowledge contained in the gain matrix K. The formula

$$b_{i+1} = b_i + K_i \, (x - Bb_i) \qquad (3.1)$$

expresses this relation. The matrix B gives a functional relationship between x and b. Two sets of Kalman biases are important for the determination of deflection changes. The sum of tilt corrections for each axis and the accelerometer biases. The procedure illustrated by fig. 3.3 combines tilt correction and accelerometer bias to obtain deflection components. No tilt corrections are made in the procedure described by fig. 3.2 and the deflections can be derived from the accelerometer biases only.

It will be shown in the next section that the use of Kalman estimation, well suited for error control, does not always give reliable results for the determination of deflection components.

4. Analysis of Results

The data used in this analysis have been provided by the Geodetic Survey of Canada. They were taken during a campaign in the Okanagan Valley of the Canadian Rocky Mountains in 1975. Fig. 4.1 shows the survey line which is a paved road between Curve and Bottom and unpaved between Bottom and Kobau. All stations marked by a triangle have astronomically determined deflections of the vertical. The height profile is shown in fig. 4.2. It should be noted that a rather extreme terrain has been selected with a number of sharp curves in the second part of the line and a height difference of about 1600 m.

The surveys were made by car during a period of about three weeks in May and June and usually a forward and a backward running were made with one alignment. The method used is that described by Fig. 3.3. Not all legs of the traverse were observed with the same frequency; the minimum number of double runs was 5 the maximum number 10, with an average of about 8 runs.

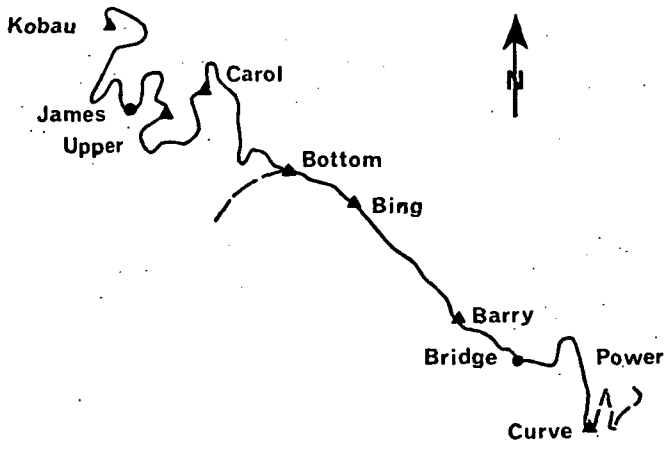

Fig. 4.1 Map of the survey route

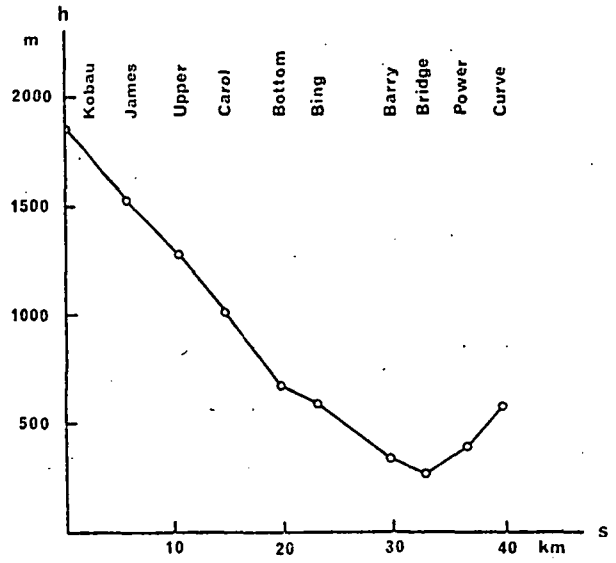

Fig. 4.2 Topographic profile of the survey route

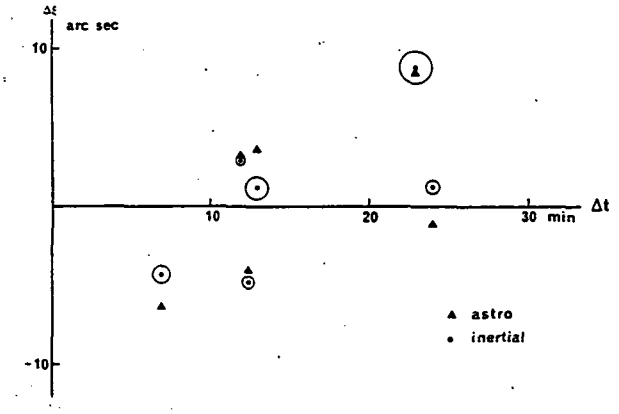

Fig. 4.3 Accuracy of system derived $\Delta\xi$ - values

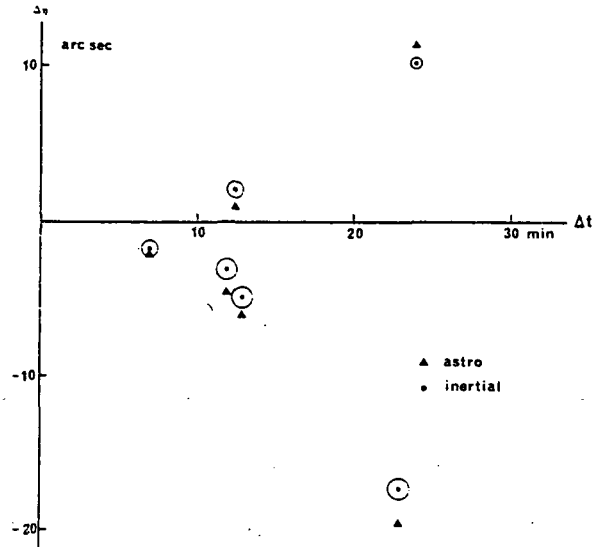

Fig. 4.4 Accuracy of system derived Δη - values

Since only the differences Δξ and Δη between stations can be determined, the most obvious approach is to compute these differences and to estimate standard deviations for each difference. Since sample sizes were rather small in some cases, the hypothesis was tested if all variances could be considered as representing the same population. The standard deviations of Δξ and Δη were almost identical with $\sigma_{\Delta\xi} = \pm$ 0".54 and $\sigma_{\Delta\eta} = \pm$ 0".56, so that the standard error for a deflection difference could be estimated from a sample size of about 100. The result was

$$\sigma_I = \pm 0".55$$

for the mean of a forward and a backward running. The standard deviations of the individual differences were compared to σ_I and all except one passed the F-test on a 5% - level. The one rejected standard error was too small. These results show that deflection differences can be determined with a high precision. This means that the repeatability of the results is very good.

As to the accuracy fig. 4.3 and 4.4 should be consulted. They show the deflection differences as functions of the travel time Δt between stations. Mean values of the system determined differences are marked by a dot, while the differences of the astronomical deflections are represented by a triangle. The individual standard errors (1σ) are indicated by a circle. No standard deviations were available for the astronomically determined differences but judging from the observation method they should in general be below 0".5. We will therefore use

$$\sigma_A = \pm 0".5$$

as standard deviation of the astronomically determined differences.

The figures show very clearly that the deviations between astronomically determined and system derived differences is much larger than could be expected from the standard deviations. The standard error σ_{A-I} (astronomical - inertial) is

$$\sigma_{A-I} = \pm 1".73 .$$

Considering the size of the deflection differences it can be concluded that the inertial system recovers deflection changes with a good accuracy. Considering the size of σ_I and σ_A it must be concluded that there are systematic differences between the two data groups. Although σ_I and σ_A are almost equal there is some reason to believe that the differences derived from the inertial system are systematically wrong. One indication is given by the large differences between forward and backward runnings.

If we compute the mean of the differences between stations using only forward runs in one case and only backward runs in the other we obtain the results summarized in table 4.1.

The standard deviations σ_F and σ_B belong to the means of the forward and the backward runs respectively. The standard deviations σ_{F-B} characterize the deviations between the individual forward and backward runs. The sample size is about 50 in each case. Using an F-test at a 5% - level it must be concluded that there are systematic deviations between the forward and backward runnings.

Part of these differences can be explained by the 'slowness' of the Kalman estimation to adapt to a new situation. If we look at formula (3.1)

$$b_{i+1} = b_i + K_i\ (x - Bb_i) \qquad (3.1)$$

the new estimate b_{i+1} is composed of the old estimate b_i and a portion representing the influence of the new data. This influence is weighted by the gain matrix K which is dependent on the a priori correlation function and previous estimates. Thus, the old estimate b_i may to a large extent determine the value of b_{i+1}, i.e. the estimation is somewhat slow to follow changes in the value of b. The situation is illustrated in fig. 4.5 The full line represents a deflection profile, the dashed line its estimation by the Kalman procedure when coming from the left side. There is a kind of 'overshooting' due to the influence of the old estimate which makes the difference P_2P_3 too small. When coming from the right side P_2P_3 will be determined correctly but in this case P_1P_2 will be wrong. This explains the differences between forward and backward runnings. The following example will demonstrate that this effect is

Deflection Component	σ_{F-B}	σ_F	σ_B
Δξ	± 1.43	± 0.64	± 0.96
Δη	± 3.86	± 1.12	± 1.03

Table 4.1 Comparison of standard deviations

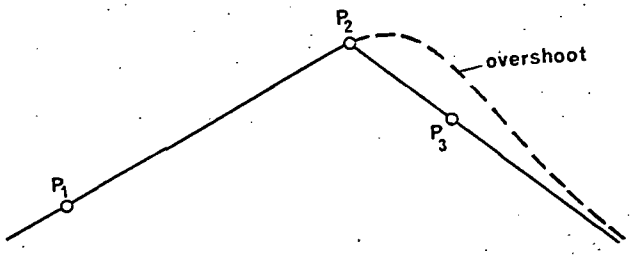

Fig. 4.5 'Overshooting' of Kalman filter

present in the data and leads to observable systematical errors.

Fig. 4.6 shows the ξ-profile between the stations Barry and Carol and outlines the Kalman estimation of the difference Bing-Bottom. Coming from Barry 'overshooting' at Bing will produce a difference which is too small. Coming from Carol 'undershooting' will also give too small a difference. The actual values determined as means of 10 measurements are

$$\Delta\xi_{BI-BO} = -4\overset{''}{.}08 \pm 0\overset{''}{.}07$$

$$\Delta\xi_{BO-BI} = -4.42 \pm 0\overset{''}{.}32$$

The 'correct' difference from astronomical observations is $\Delta\xi = -6\overset{''}{.}53$. It should be noted that the line between Bing and Bottom is rather straight and has a length of only 6.6 km. Thus, there is no other obvious explanation for errors of this size.

The interpretation of the results from the curved part of the line is more difficult. As has been shown in section 2 changes in the gradient of ξ and η are likely to occur with each change in platform heading. Thus, for lines having several sharp curves between stations the unwanted effects of the Kalman procedure may either accumulate or cancel. This is exactly the pattern which evolves for the winding part of the line. Some system derived deflection differences agree very well with those obtained from astronomical observations, others deviate by 2" to 3". It appears that these deviations are of a size which can be expected from the slow adaption of the Kalman procedure. It is difficult to say, however, if this is the main effect or if changes in thermal and magnetic gradients as functions of platform heading also play a major role in changing the drift rates and by this the deflection estimates. There is one

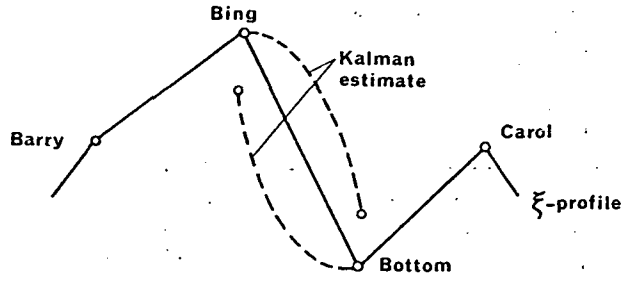

Fig. 4.6 Explanation of systematic $\Delta\xi$ - discrepancy between Bing - Bottom

observation which would indirectly confirm a highly nonlinear drift for the data analysed here. The value of $\sigma_I = \pm 0\overset{''}{.}55$ has been computed by making the usual linear drift removal between Curve and Kobau. When not removing any drift from the data the corresponding value drops to $\sigma_I' = 0\overset{''}{.}50$. This shows that the assumption of linear drift is a wrong model on a line like this because it does not improve results. Since drift is definitely present it must be suspected that it is highly nonlinear. This nonlinearity can probably be correlated to changes in platform heading.

In order to control these different effects it will be necessary to refine the mathematical model and to change the software accordingly. The gravity disturbance vector should be modelled as a position dependent quantity rather than a time dependent bias term of stochastic nature. An adequate model of the changes in gyro drift due to platform heading can probably be obtained by stationary experiments. Otherwise, a change of the measuring procedure would be necessary in order to determine drift changes during field operations.

The accuracy of deflection determination with present- day inertial instrumentation can be summarized in two numbers. Using the system as it is systematic differences of 2" to 3" must be expected even over relatively short distances. With changes in the software a standard error of ± 1" or better can be expected between stations not more than half an hour of travel time apart. It should be noted that these results have been obtained in mountainous terrain and that no restrictions with respect to the course of the survey have been imposed. Results obtained by Fishel and Roof (1977) seem to confirm the above findings.

Acknowledgements. The data analysed in this paper have been made available by the Geodetic Survey of Canada. The cooperative support of several persons in this agency is gratefully acknowledged. The paper is a contribution to the Research Agreement No. 132728 between the Department of Energy, Mines, and Resources and the University of New Brunswick.

References

Britting, K.R. (1971), Inertial Navigation Systems Analysis. Wiley-Interscience, New York.

Farrel, F.L. (1976), Integrated Aircraft Navigation. Academic Press, New York.

Fishel, N. and E. Roof (1977), Results of Tests Using an Inertial Rapid Geodetic Survey System (RGSS). Proceedings of the American Congress on Surveying and Mapping, pp. 100 - 153.

Grafarend, E. (1975), Three Dimensional Geodesy I - The Holonomity Problem. Zeitschrift für Vermessungswesen, 100, pp. 269-281.

Heiskanen, W.A. and H. Moritz (1967), Physical Geodesy. W.H. Freeman and Co., San Francisco.

Lyon, F. (1977), Optimized Method for the Derivation of the Deflections of the Vertical from RGSS Data. Proceedings of the "First International Symposium on Inertial Technology for Surveying and Geodesy", Ottawa, pp. 417-428.

Luetzow, von B. (1977), A Review of Past, Present and Future USAETL Inertial/Gradiometric Geodesy Activities and Programs. Proceedings of the "First International Symposium on Inertial Technology for Surveying and Geodesy", Ottawa, pp. 60-72.

Moritz, H. (1975), Combination of Aerial Gravimetry and Gradiometry. Report No. 223 of the Department of Geodetic Science, The Ohio State University, Columbus.

Schwarz, K.P. (1977), Airborne Inertial Systems for Gravity Determination in Ocean Areas. Proceedings of the "First International Symposium on Inertial Technology for Surveying and Geodesy", pp. 351-360.

Todd, M. (1977), The Development of the Inertial Rapid Geodetic Survey System at USAETL. Proceedings of the "First International Symposium on Inertial Technology for Surveying and Geodesy", Ottawa, pp. 113-120.